Biogeosciences, 15, 1185–1201, 2018
https://doi.org/10.5194/bg-15-1185-2018

Biogeosciences Open Access EGU

Smaller global and regional carbon emissions from gross land use change when considering sub-grid secondary land cohorts in a global dynamic vegetation model

Chao Yue, Philippe Ciais, and Wei Li

Laboratoire des Sciences du Climat et de l'Environnement, LSCE/IPSL, CEA-CNRS-UVSQ, Université Paris-Saclay, 91191 Gif-sur-Yvette, France

Correspondence: Chao Yue (chao.yue@lsce.ipsl.fr)

Received: 26 July 2017 – Discussion started: 4 September 2017
Revised: 21 January 2018 – Accepted: 24 January 2018 – Published: 27 February 2018

Abstract. Several modelling studies reported elevated carbon emissions from historical land use change (E_{LUC}) by including bidirectional transitions on the sub-grid scale (termed gross land use change), dominated by shifting cultivation and other land turnover processes. However, most dynamic global vegetation models (DGVMs) that have implemented gross land use change either do not account for sub-grid secondary lands, or often have only one single secondary land tile over a model grid cell and thus cannot account for various rotation lengths in shifting cultivation and associated secondary forest age dynamics. Therefore, it remains uncertain how realistic the past E_{LUC} estimations are and how estimated E_{LUC} will differ between the two modelling approaches with and without multiple sub-grid secondary land cohorts – in particular secondary forest cohorts. Here we investigated historical E_{LUC} over 1501–2005 by including sub-grid forest age dynamics in a DGVM. We run two simulations, one with no secondary forests ($S_{ageless}$) and the other with sub-grid secondary forests of six age classes whose demography is driven by historical land use change (S_{age}). Estimated global E_{LUC} for 1501–2005 is 176 Pg C in S_{age} compared to 197 Pg C in $S_{ageless}$. The lower E_{LUC} values in S_{age} arise mainly from shifting cultivation in the tropics under an assumed constant rotation length of 15 years, being 27 Pg C in S_{age} in contrast to 46 Pg C in $S_{ageless}$. Estimated cumulative E_{LUC} values from wood harvest in the S_{age} simulation (31 Pg C) are however slightly higher than $S_{ageless}$ (27 Pg C) when the model is forced by reconstructed harvested areas because secondary forests targeted in S_{age} for harvest priority are insufficient to meet the prescribed harvest area, leading to wood harvest being dominated by old primary forests. An alternative approach to quantify wood harvest E_{LUC}, i.e. always harvesting the close-to-mature forests in both $S_{ageless}$ and S_{age}, yields similar values of 33 Pg C by both simulations. The lower E_{LUC} from shifting cultivation in S_{age} simulations depends on the predefined forest clearing priority rules in the model and the assumed rotation length. A set of sensitivity model runs over Africa reveal that a longer rotation length over the historical period likely results in higher emissions. Our results highlight that although gross land use change as a former missing emission component is included by a growing number of DGVMs, its contribution to overall E_{LUC} remains uncertain and tends to be overestimated when models ignore sub-grid secondary forests.

1 Introduction

Historical land use change (LUC), such as the permanent establishment of agricultural land over forests (deforestation), shifting cultivation, and wood harvest, has contributed significantly to the atmospheric CO_2 increase, in particular since industrialization (Houghton, 2003; Le Quéré et al., 2016; Pongratz et al., 2009). Carbon emissions from land use change (E_{LUC}) are often defined as the net effect between carbon release on newly disturbed lands, given that in most cases newly created lands have a lower carbon density than natural ecosystems (e.g. deforestation or forest degradation), and carbon uptake on recovering ecosystems (e.g. cropland abandonment, afforestation, or reforestation). As the high spatial heterogeneity of land conversions

precludes any direct measurements of global or regional E_{LUC}, modelling turned out to be the only approach to its quantification (Gasser and Ciais, 2013; Hansis et al., 2015; Houghton, 1999, 2003; Piao et al., 2009b). Methods to quantify E_{LUC} could fall broadly into three categories, namely bookkeeping models (Gasser and Ciais, 2013; Hansis et al., 2015; Houghton, 2003), dynamic global vegetation models (DGVMs; Shevliakova et al., 2009; Stocker et al., 2014; Wilkenskjeld et al., 2014; Yang et al., 2010), and satellite-based estimates of deforestation fluxes (Baccini et al., 2012; van der Werf et al., 2010).

When including sub-grid bidirectional gross LUCs such as shifting cultivation or other forms of land turnover processes, models are found to yield higher estimates of E_{LUC} for 1850–2005 by 2–38 % than accounting for net transitions only (Hansis et al., 2015). Wood harvest, although it does not change the underlying land use type, can also lead to additional carbon emissions due to fast carbon release from recently harvested forests and slow uptake from regrowing ones (Shevliakova et al., 2009; Stocker et al., 2014). Because of their importance in estimating historical LUC emissions, gross LUC and wood harvest have been implemented in several DGVMs, as synthesized in the Table 1 of Yue et al. (2018). A recent synthesis study by Arneth et al. (2017) reported a consistent increase in E_{LUC} by several models when including shifting cultivation and wood harvest, as well as other agricultural management processes such as pasture harvest and cropland management. These processes altogether yield an upward shift in estimated historical E_{LUC}, implying a larger potential in the land-based mitigation in the future if deforestation or forest degradation can be stopped.

While replacing forest with cropland or pasture typically leads to carbon release, afforestation and forest regrowth following harvest or agricultural abandonment sequester carbon in growing biomass stocks. Some recent studies, on both site (Poorter et al., 2016) and regional scales (Chazdon et al., 2016), show that secondary forests recovering from historical LUC are contributing to the terrestrial carbon uptake, and that the carbon stored per unit land sometimes exceeds that of primary forests (Poorter et al., 2016). While explicit representation of sub-grid secondary forests and other lands with different years since the last disturbance (defined as cohorts or age classes) is straightforward in bookkeeping models (Hansis et al., 2015), and is fairly easy in some DGVMs combined with a forest gap model (e.g. LPJ-GUESS; Bayer et al., 2017), only a few DGVMs following an "area-based" approach (Smith et al., 2001) have done this but usually with a single secondary cohort for a given vegetation type (Yue et al., 2018). Shevliakova et al. (2009) pioneered the inclusion of both gross LUC and secondary lands in a DGVM. Their model can contain up to a total of 12 secondary land cohorts, but the spatial separation of natural plant functional types (PFTs) were limited. In some other DGVMs (Kato et al., 2013; Stocker et al., 2014; Yang et al., 2010), secondary lands were limited to have one cohort per PFT. This has limited the accurate representation of the carbon balance in differently aged secondary forests.

In reality, shifting cultivation and wood harvest (forestry) tend to have certain rotation lengths (McGrath et al., 2015; van Vliet et al., 2012), which vary among different regions and management systems. Simulating these LUC activities by targeting forests with an appropriate age can have important consequences in derived E_{LUC} since young vs. old forests have very different aboveground biomass stocks. Using a bookkeeping model, Hansis et al. (2015) showed that assuming only secondary land clearing in gross change yields a 2 % increase in E_{LUC} compared with accounting for net transitions only, much smaller than the 24 % increase when assuming primary land clearing as a priority in gross change. Worldwide, systematic information on historical and present rotation lengths of shifting cultivation and wood harvest is missing. Some LUC reconstructions, such as the land-use harmonization version 1 (LUH1) data (Hurtt et al., 2011), assumed a fixed rotation length of 15 years for shifting agriculture in the tropics, and this assumption has been used in some modelling studies (Bayer et al., 2017).

Past studies using DGVMs mainly focused different estimates of E_{LUC} between accounting for gross LUC and net transitions only. Very few studies have addressed the issue of how much E_{LUC} from gross transitions differs by assuming clearing of primary forests vs. secondary forests. The former issue can be tackled by DGVMs without sub-grid secondary lands, while the latter one can only be addressed by DGVMs with an explicit sub-grid secondary land age structure. Furthermore, it is also unclear how large the impact of shifting cultivation rotation length on the estimated E_{LUC} is.

In this study, we quantify global and regional carbon emissions from historical gross LUC since 1501 using a global vegetation model ORCHIDEE (ORganizing Carbon and Hydrology In Dynamic EcosystEms). The ORCHIDEE model has recently incorporated gross LUC and wood harvest, along with the representation of sub-grid secondary land cohorts. The model development and examination of model behaviour on site and regional scales are documented in a companion paper (Yue et al., 2018). The current paper focuses on the model global application. Our objectives are (1) to quantify global and regional carbon emissions from historical gross LUC since 1501 and to examine the differences in E_{LUC} when considering sub-grid secondary land cohorts by using parallel model simulations; (2) to examine contributions to E_{LUC} from different LUC processes (i.e. net transitions only, shifting cultivation or land turnover, and wood harvest) and how they differ between the two model configurations with and without secondary land cohorts; and (3) to examine the impacts of different rotation lengths in shifting cultivation on E_{LUC}. Hereafter, we will use the terms "shifting cultivation" or "land turnover" interchangeably as they refer to the same process in the model – bidirectional equal-area land transitions between two land use types.

2 Methods

2.1 ORCHIDEE-MICT model v8.4.2 and the implemented gross LUC processes

ORCHIDEE (Krinner et al., 2005) is a DGVM and the land surface component of the IPSL Earth system model. It comprises three sub-models that operate on different time steps. The SECHIBA sub-model operates on half-hourly time steps and simulates fast exchanges of energy, water, and momentum between vegetation and the atmosphere. The STOMATE sub-model operates on daily time steps and simulates vegetation carbon cycle processes including photosynthate allocation, plant phenology, vegetation mortality, and recruitment. The third sub-model contains various modules of different processes on varying time steps, such as vegetation dynamics, fire disturbance, and LUC.

The LUC module in ORCHIDEE was originally developed in Piao et al. (2009a), in which only net transitions were taken into account. Recently, a gross LUC module, together with explicit representation of differently aged sub-grid land cohorts, has been implemented in a branch of the ORCHIDEE model known as ORCHIDEE-MICT (Yue et al., 2018). This model will be henceforth referred to as ORCHIDEE-MICT v8.4.2. Idealized site-scale simulations with this model have shown that estimated carbon emissions from shifting cultivation and wood harvest are reduced by explicitly including sub-grid age dynamics, in comparison with an alternative approach to representing land cover types with a single ageless patch. This is because the secondary forests that are cleared in shifting cultivation or wood harvest with a rotation length of 15 years have a lower biomass than the mature forests that are otherwise cleared. Yue et al. (2018) provides details on the underlying processes in explaining differences in E_{LUC} regarding whether sub-grid forest age structure is considered or not.

The gross LUC module operates on an annual time step. For the very first year of the simulation, an initial land cover map (represented as a map of PFTs) is prescribed. Land cover maps of subsequent years are updated using land use transition matrices corresponding to different LUC processes. Land use transitions between four vegetated land cover types are included: forest, natural grassland, pasture, and cropland. The model separates overall LUC into three additive subprocesses in order to diagnose their individual contributions to E_{LUC}, namely net LUC equivalent to the original approach that considers net transitions only, land turnover equivalent to shifting cultivation, and wood harvest. Matrices for net LUC and land turnover ($[X_{i,j}]$) take the form of four rows by four columns, with $X_{i,j}$ indicating the land transition from vegetation type i to j. The matrix for wood harvest has only two elements, indicating forest area as grid cell fractions that are subject to harvest from primary and secondary forests. The current model version assumes that bare land fraction remains constant throughout the entire simulation.

Differentiation of age classes applies to all vegetation types in the model. The number of age classes for each PFT can be customized via a configuration file. Age classes for forest PFTs are distinguished in terms of woody biomass, while those for herbaceous PFTs are defined using soil carbon stock. Newly established lands after LUC are assigned to the youngest age class. Forest cohorts move to the next age class when their woody biomass exceeds the threshold. For herbaceous PFTs, younger age classes are parameterized to have a larger soil carbon stock. This serves mainly as a preliminary attempt to have cohorts of secondary lands for herbaceous vegetation. Because the change in soil carbon depends on the vegetation types before and after LUC and on climate conditions (Don et al., 2011; Poeplau et al., 2011), ideally agricultural cohorts from different origins should be differentiated, with an origin-specific soil carbon boundary parameterization. However, to avoid inflating the total number of cohorts and the associated computational demand, as a first attempt here, we simply divided each herbaceous PFT into two broad sub-grid cohorts according to their soil carbon stocks and without considering their individual origins. We expect that such a parameterization can accommodate some typical LUC processes, such as the conversion of forest to cropland where soil carbon usually decreases over time, but not all LUC types (for instance, soil carbon stock increases when a forest is converted to a pasture).

To simulate LUC with sub-grid land cohorts, a set of priority rules become necessary regarding which land cohorts to target given a specific LUC type (Table 1 in Yue et al., 2018) and regarding how to allocate LUC area into different PFTs of the same age class. For net LUC, clearing of forests exclusively starts from the oldest cohort and then moves onto younger ones until the youngest one. For shifting cultivation or land turnover, forest clearing starts from a predefined middle-aged class, and then moves onto older ones if this starting age class is used up, until the oldest ones. The primary target forest cohort in shifting cultivation and secondary forest harvest can be parameterized in the model. For the current study, shifting cultivation primarily targets the third-youngest cohort (Cohort_3) and secondary forest harvest primarily targets the second-youngest cohort (Cohort_2), with a total number of six forest cohorts (Cohort_1 to Cohort_6, with Cohort_1 being the youngest) being simulated. This is to accommodate the assumption used in the LUC forcing data that shifting cultivation has a certain rotation length (see the Sect. 2.2), so that secondary forests are given a high priority to be cleared for agricultural land, and older forests will be cleared when even more agricultural lands are needed. Finally, for all other land cover types that are used as a source for conversion, as well as for primary forest harvest, we start from the oldest age class and move sequentially to younger ones in order to meet the prescribed LUC area in the forcing data. After the LUC area is allocated on the cohort level, it is then distributed among different PFTs in proportion to their existing areas in this cohort.

In order to compare the simulated E_{LUC} with and without sub-grid secondary land cohorts, ORCHIDEE-MICT v8.4.2 can be run in a way that each PFT has one single age class. This is equivalent to the alternative approach by which no sub-grid land cohorts are simulated. For more information on the rationale and details of LUC implementation in ORCHIDEE-MICT v8.4.2, readers are referred to Yue et al. (2018).

2.2 Preparation of forcing LUC matrices

For historical land use transitions, the land use harmonized data set version 1 (LUH1) for the CMIP5 project was used (Hurtt et al., 2011, http://luh.umd.edu/data.shtml#LUH1_Data). We used the version of LUH1 data without urban lands as ORCHIDEE-MICT v8.4.2 does not simulate the effects of urban lands. The original data set is at a 0.5° spatial resolution with an annual time step covering 1500–2005. Four land use types are included: primary natural land, secondary natural land, pasture, and cropland. The type natural land consists of grassland and forest (which are separated in ORCHIDEE-MICT) but their relative fractions are not separated. In LUH1, land use transitions from either primary or secondary natural land to pasture or cropland are provided, and vice versa. Secondary natural lands originated from pasture or cropland abandonment. In addition, land use transitions between pasture and cropland are provided as well. Harvested wood comes either from primary or secondary forest or non-forest lands, with ground area fractions that are harvested being available. Note that this does not contradict the fact that forest and grassland fractions are not separated within the land use type natural land because forests are defined as natural lands with a certain biomass carbon stock based on the simulated biomass in a terrestrial model (Hurtt et al., 2011).

Rather than the simple terrestrial model (Miami-LU) used in Hurtt et al. (2011) to separate natural vegetation into forested and non-forest land, ORCHIDEE-MICT distinguishes eight forest PFTs, two natural grassland PFTs, two cropland PFTs (Krinner et al., 2005), and two pasture PFTs. Thus, to use LUH1 reconstructions as a forcing input, assumptions have to be made to disaggregate LUH1 land use types into corresponding ORCHIDEE PFTs. For this purpose, we used an ORCHIDEE-compatible PFT map generated from the European Space Agency (ESA) Climate Change Initiative (CCI) land cover map (shortened as the ESA-CCI-LC map) covering a 5-year period of 2003–2007 (European Space Agency, 2014), assuming that it corresponds to the land use distribution for 2005 by the LUH1 data. Subsequently, we backcast historical PFT map time series for 1500–2004 based on this 2005 PFT map using LUH1 historical net land use transitions as a constraint. Because land turnover involves an equal, bidirectional land transition between two land cover types, it does not lead to any net annual changes in the PFT map. Therefore, only net transition information is needed when backcasting historical PFT maps.

To separate land use transitions in LUH1 into processes of net LUC and land turnover, we simply treat net LUC as the land transitions excluding the minimum reverse fluxes between two land use types. During the backcasting process, reconciliations have to be made where LUH1 data disagree with the ESA map on the grid cell scale. When backcasting historical PFT map time series using net LUC matrices, we assume that when pasture or cropland is created, they come from an equal share of forest and grassland; when their fractions decrease, cropland abandonment leads first to forest recovery and is then followed by natural grassland expansion, while pasture abandonment leads to an equal share of forest and natural grassland expansion. We then treat the minimum of two reverse land fluxes between secondary natural land and cropland or pasture as land turnover transitions. For each year, the land turnover transition between two land use types is not allowed to exceed the minimum of their existing areas. Spatially resolved forest harvest time series are provided in LUH1. We built the wood harvest matrices by limiting wood harvest area within the total area of forest PFTs over each grid cell for each year. Primary and secondary forest wood harvests from LUH1 were included and treated as primary and secondary forest harvest in the model, respectively, with non-forest wood harvest being discarded. More details on PFT map backcasting and the construction of land use transition matrices are provided in the Supplement.

The construction of historical PFT maps and land transition matrices was performed at 2° resolution for the whole globe, after resampling all input data from their original resolution to 2°. The reconstructed global forest area agrees with that by Peng et al. (2017), who have backcast historical ORCHIDEE PFT map series using the same ESA-CCI-LC 2005 PFT map and historical pasture and crop distributions from LUH1 but not the LUH1 land use transitions, with historical forest areas in the nine regions of the globe being constrained by data in Houghton (2003) based on national forest area statistics. The land turnover transitions between secondary land (forest and grassland) and cropland (or pasture) from the matrices defined above are smaller than originally prescribed in LUH1 because some of the prescribed transitions are ignored due to the inconsistency between LUH1 map in 2005 and the 2005 ORCHIDEE PFT map (see Supplement for detailed comparison). Because of this inconsistency, around 35 % of net transitions from natural land to pasture, and 14 % of net transitions from natural land to cropland, were omitted when adapting the LUH1 data set to our model. About 20 % of the turnover transitions between secondary land and pasture were omitted, and 11 % of turnover transitions between secondary land and cropland were omitted. Such inconsistencies among different data sets are a rather common challenge for their application in DGVMs, which have been reported by, for example, Li et al. (2018), Meiyappan and Jain (2012), and Peng et al. (2017). Note that shifting cultivation (land

turnover) is limited to the tropical band as in LUH1, and the land turnover change resulting from the gridded LUH1 data upscaling from 0.5° to 2° is not included. The missing land turnover areas represent 17 % of the turnover between natural lands and cropland that is included in our study, and 14 % of the turnovers between natural lands and pasture.

2.3 Simulation protocol

2.3.1 Separate contributions of different LUC processes

The PFT map of year 1500 as generated from the backcasting procedure (see the previous section) was used during the model spin-up. Climate data included CRUNCEP v5.3.2 climate forcing at 2° resolution covering 1901–2013. For the spin-up, climate data were cycled from 1901 to 1910, with atmospheric CO_2 concentration being fixed at the 1750 level (277 ppm). Following LUH1 (Hurtt et al., 2011), we assume that no LUC occurs during the model spin-up. This might lead to overestimation of E_{LUC} for the beginning years of the transient simulation due to high carbon stocks that are free from LUC before 1501. Conversely, legacy emissions from LUC activities before 1501 are also omitted. In general, because the magnitude of annual LUC activities for 1501–1520 is very small (Fig. 2), we assume that the bias in E_{LUC} induced by not including LUC in the spin-up is small. In addition, simulated E_{LUC} is less influenced by this factor after ca. 1700, which dominates the cumulative E_{LUC} since 1501. The spin-up lasts for 450 years and includes a specific accelerated soil carbon module to speed up the equilibrium of soil carbon stock. Fires and fire carbon emissions are simulated with a prognostic fire module (Yue et al., 2014), with fire occurring only on forests and natural grasslands. Simulated net land–atmosphere carbon flux is calculated as net biome production (NBP):

$$\mathrm{NBP} = \mathrm{NPP} - F_{\mathrm{Inst}} - F_{\mathrm{Wood}} - F_{\mathrm{HR}} - F_{\mathrm{Fire}} - F_{\mathrm{AH}} - F_{\mathrm{pasture}}, \quad (1)$$

where NPP is the net primary production. All fluxes starting with "F" are outward fluxes (i.e. carbon fluxes from ecosystems to the atmosphere), with F_{Inst} being instantaneous carbon fluxes lost during LUC (e.g. site preparation, deforestation fires); F_{Wood} delayed carbon emissions from the degradation of harvested wood product pools; F_{HR} soil respiration; F_{Fire} carbon emissions from natural and anthropogenic open vegetation fires; F_{AH} carbon emissions from agricultural harvest, including harvest from croplands and pastures (treated as a carbon source for the year of harvest equaling the harvested biomass; this source is assumed to occur over the grid cell being harvested, ignoring the transport, processing, and final consumption of agricultural yield); and F_{pasture} additional non-harvest carbon sources from pastures including export of animal milk and methane emissions. E_{LUC} is quantified as the differences in NBP between simulations without and with LUC, with positive values representing carbon sources.

We conducted a set of additive factorial simulations (S0 to S3) by including matrices of different LUC processes in each simulation (Table 1), which allows diagnosis of E_{LUC} from different LUC processes. Note that this separation is carried out from a theoretical point of view with the objective to investigate the impacts on E_{LUC} from gross LUC when including sub-grid multiple land cohorts. The simulations of S0 to S3 allow separation of the contributions to E_{LUC} by different LUC processes in a fully additive manner and this works accurately for a linear system. To test the uncertainties in $E_{\mathrm{LUC\ turnover}}$ and $E_{\mathrm{LUC\ harvest}}$ introduced by this assumption, we performed an alternative S2b simulation, which includes net LUC and wood harvest. $E_{\mathrm{LUC\ turnover}}$ and $E_{\mathrm{LUC\ harvest}}$ are then calculated using both S2 and S2b simulations, and emissions from these two factorial runs are compared with each other. Henceforth for briefness, we denote the simulation without sub-grid age class dynamics as $\mathrm{S_{ageless}}$ and the simulation with sub-grid age dynamics as $\mathrm{S_{age}}$. At last, to investigate the sensitivity of $E_{\mathrm{LUC\ turnover}}$ to shifting cultivation rotation length, we performed further simulations for Africa as a case study. Another five simulations were branched from the S2 simulation starting from the year 1860, in which the primary target cohort for land turnover was varied as each of the five cohorts other than $\mathrm{Cohort_3}$, the default primary target cohort for land turnover.

2.3.2 Define thresholds for age classes

For the simulation with age dynamics ($\mathrm{S_{age}}$), six age classes are used for forest PFTs and two age classes for other PFTs. As explained, age classes of forest PFTs are separated in terms of woody biomass. The LUH1 data assume a 15-year residence time for agricultural land in shifting cultivation in tropical regions. Ideally, model parameterization of woody biomass thresholds should allow corresponding forest age to be inferred, so that clearing of forest age class in the model could match that in the LUH1 data set. For this purpose, we fit a woody biomass–age curve for each forest PFT using the model data from the spin-up:

$$B = B_{\mathrm{max}} \cdot [1 - \exp(-k \cdot \ \mathrm{age})], \quad (2)$$

where B_{max} is the asymptotic maximum woody biomass; k is the biomass turnover rate (yr^{-1}). The curve fitting used PFT-specific woody biomass time series during spin-up by averaging all grid cells across the globe. The ratios of woody biomass thresholds for each age class to the maximum woody biomass (B_{max}) are looked up from this curve, based on their corresponding forest ages (Table 2). Next, these ratios are multiplied with the equilibrium woody biomass at each grid cell, approximated by the woody biomass at the end of model spin-up, to derive a spatial map of thresholds in woody biomass. We set the corresponding age for the $\mathrm{Cohort_3}$ for tropical forests as 15 years, in line with the res-

Table 1. Factorial simulations to quantify E_{LUC} from each of the LUC processes considered: net land use change ($E_{LUC\ net}$), land turnover ($E_{LUC\ turnover}$), and wood harvest ($E_{LUC\ harvest}$), with $E_{LUC\ all}$ being carbon emissions from all three processes. The plus signs (+) indicate that the process in question is included, with $S0_{ageless}$ ($S0_{age}$) having no LUC activities to $S3_{ageless}$ ($S3_{age}$) including all LUC processes. E_{LUC} is quantified as the difference in net biome production (NBP) between simulations without and with LUC. To explore the uncertainties by using a fully additive approach, we included an alternative S2b simulation, which includes net land use change and land turnover. $E_{LUC\ turnover}$ and $E_{LUC\ harvest}$ are consequently calculated using this alternative simulation as well.

Simulations and LUC processes included			
Simulations	Net land use change	Land turnover	Wood harvest
$S0_{ageless}$ ($S0_{age}$)			
$S1_{ageless}$ ($S1_{age}$)	+		
$S2_{ageless}$ ($S2_{age}$)	+	+	
$S3_{ageless}$ ($S3_{age}$)	+	+	+
$S2b_{ageless}$ ($S2b_{age}$)	+		+
Calculation of E_{LUC}			
No age dynamics ($S_{ageless}$)		With age dynamics (S_{age})	
$E_{LUC\ net,\ ageless} = NBP_{S0,\ ageless} - NBP_{S1,\ ageless}$		$E_{LUC\ net,\ age} = NBP_{S0,\ age} - NBP_{S1,\ age}$	
$E_{LUC\ turnover,\ ageless} = NBP_{S1,\ ageless} - NBP_{S2,\ ageless}$		$E_{LUC\ turnover,\ age} = NBP_{S1,\ age} - NBP_{S2,\ age}$	
$E_{LUC\ harvest,\ ageless} = NBP_{S2,\ ageless} - NBP_{S3,\ ageless}$		$E_{LUC\ harvest,\ age} = NBP_{S2,\ age} - NBP_{S3,\ age}$	
$E_{LUC\ turnover,\ ageless\ S2b} = NBP_{S2b,\ ageless} - NBP_{S3,\ ageless}$		$E_{LUC\ turnover,\ age\ S2b} = NBP_{S2b,\ age} - NBP_{S3,\ age}$	
$E_{LUC\ harvest,\ ageless\ S2b} = NBP_{S1,\ ageless} - NBP_{S2b,\ ageless}$		$E_{LUC\ harvest,\ age\ S2b} = NBP_{S1,\ age} - NBP_{S2b,\ age}$	
$E_{LUC\ all,\ ageless} = NBP_{S0,\ ageless} - NBP_{S3,\ ageless}$		$E_{LUC\ all,\ age} = NBP_{S0,\ age} - NBP_{S3,\ age}$	

Table 2. Determination of woody biomass thresholds for different age classes of forest PFTs. We first look up through the biomass–age curve (Eq. 2) for a ratio of woody biomass to the maximum biomass that corresponds to certain ages (years), and then we multiply this ratio with equilibrium biomass at the end of spin-up for each grid cell. Numbers in the table indicate the ratio of woody biomass to the maximum woody biomass (B_{max} in Eq. 2), and the numbers in parentheses indicate the corresponding forest age.

Forest cohorts	Tropical forest	Temperate forest	Boreal forest
Age1	0.1 (3 year)	0.07 (3 year)	0.04 (3 year)
Age2	0.26 (9 year)	0.22 (10 year)	0.19 (15 year)
Age3	0.39 (15 year)	0.40 (20 year)	0.34 (30 year)
Age4	0.6 (27 year)	0.6 (35 year)	0.6 (65 year)
Age5	0.8 (48 year)	0.8 (64 year)	0.8 (114 year)
Age6	1.2 (> 48 year)	1.2 (> 64 year)	1.2 (> 114 year)

idence time of shifting cultivation assumed in LUH1. Considering that temperate and boreal forests grow slower than tropical ones, forest ages corresponding to the $Cohort_3$ are set as 20 and 30 years for temperate and boreal forests, respectively.

We acknowledge that using such static woody biomass boundaries cannot ensure a forest of an exact given age to be cleared in the transient simulations because changes in environmental conditions (e.g. atmospheric CO_2 concentrations, climate) may alter the woody biomass–age curves established from the spin-up results. For example, the boundary biomass limits may be reached at an earlier age in case productivity increases due to changes in environmental conditions. If we assume that land managers always clear forest according to their ages, then our simulated E_{LUC} might be underestimated, provided there is a higher biomass for a given age in transient simulations than that, in the spin-up. But the uncertainties resulting from using static biomass boundaries should be less influential than the uncertainty induced by the fact that in general, rotational lengths of land turnover are poorly known and that a constant 15-year length for shifting agriculture in tropical regions is assumed (Hurtt et al., 2011). For wood harvest, we also assumed three different fixed rotation lengths for boreal, temperate, and tropical regions (Table 2).

We used two age classes for each herbaceous PFT including natural grassland and cropland and pasture, representing high vs. low soil carbon densities, respectively. The energy balance in ORCHIDEE-MICT v8.4.2 is resolved over the whole grid cell, and the hydrological balance is calculated over sub-grid soil tiles (bare soil, forest, and herbs) rather than over each PFT. We thus expect the factors influencing

Table 3. Cumulative E_{LUC} for 1501–2005 (Pg C) from different processes quantified by different approaches (see Table 1 for detailed calculations of various E_{LUC} values).

	No age dynamics	With age dynamics	Emission change in S_{age} relative to $S_{ageless}$ (%)
$E_{LUC\ net}$	123.7	118.0	−4.6 %
$E_{LUC\ turnover}$	45.4	27.3	−40 %
$E_{LUC\ turnover\ S2b}$	39.9	25.1	−37 %
$E_{LUC\ harvest}$	27.4	30.8	12 %
$E_{LUC\ harvest\ S2b}$	32.9	33.0	0.0 %
$E_{LUC\ all}$	196.5	176.1	10 %

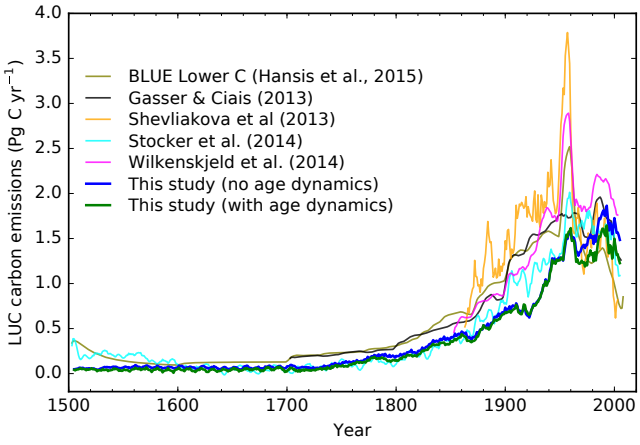

Figure 1. Annual carbon emissions from historical land use change over the globe by our studies and from other previous studies. Results of this study are smoothed using a 10-year average moving window; data of other studies are from Fig. 5 (Hansis et al., 2015) and are smoothed using a 5-year moving average window.

soil carbon decomposition (i.e. soil temperature, soil moisture) to have little difference between different age classes of the same PFTs. This justifies the small number of age classes for herbaceous PFTs selected here as it can maximize computing efficiency. Overall, this feature of separating herbaceous PFTs into multiple cohorts is coded more as a "placeholder" for the current stage of model development. Fully tracking soil carbon stocks of different vegetation types and their transient changes following LUC would require a much larger number of cohorts than that used in this study.

In S_{age} simulations, clearing of forest in the process of land turnover starts from $Cohort_3$, corresponding to 15-year-old forest, and forest clearing for wood harvest starts from $Cohort_2$. Wood product pools resulting from net LUC and land turnover and those from wood harvest are tracked separately in the model. However, land patches created from different LUC activities are not tracked individually, e.g. young forests, either re-established from land turnover or wood harvest, are merged together. In this approach, it is not possible to attribute the carbon fluxes into exact individual LUC processes, which explains why factorial simulations are needed. Within the model, the wood harvest module is executed before the modules of net LUC and land turnover. This is reasonable as a forest might be harvested prior to being converted to agricultural land. Last, we turned off the dynamic vegetation module because allowing dynamic vegetation and using prescribed backcast historical land cover maps are internally inconsistent.

3 Results

3.1 Global carbon emissions with and without sub-grid age dynamics

Cumulative E_{LUC} values during 1501–2005 for different LUC processes and model configurations are shown in Table 3. The model simulates a cumulative $E_{LUC\ net}$ of 123.7 and 118.0 Pg C during 1501–2005, for cases without and with sub-grid age dynamics, respectively. Including land turnover and wood harvest yields additional carbon emissions, with the cumulative $E_{LUC\ turnover}$ as 45.4 Pg C and $E_{LUC\ harvest}$ as 27.4 Pg C in $S_{ageless}$ simulations. Accounting for age dynamics, in contrast, generates a $E_{LUC\ turnover}$ of 27.3 Pg C, 40 % lower than that obtained by the $S_{ageless}$ simulation. The cumulative $E_{LUC\ harvest}$ for S_{age} equals 30.8 Pg C and is slightly higher than in $S_{ageless}$. When wood harvest is included on top of only the net LUC (the S2b simulation), the $E_{LUC\ harvest\ S2b}$ obtained by differing S1 and S2b simulations is slightly higher than that when wood harvest is included as the last term (i.e. quantified by differing S2 and S3 simulations). This is reasonable because in the latter case forests subject to wood harvest were already under disturbances of both land turnover and net LUC, which reduce forest biomass carbon stocks for harvest. The $E_{LUC\ turnover}$ derived from S2b simulations, in contrast, is lower than that derived from S2 simulations (Table 3). Nonetheless, a consistently lower $E_{LUC\ turnover}$ is obtained by accounting for sub-grid age dynamics, by 40 or 37 % depending on whether the S2 or S2b simulations are used. Furthermore, different estimations of $E_{LUC\ turnover}$ derived from S2 and S2b simulations are close to each other, with a difference of $\sim$ 10 % of their mean value, indicating that LUC emissions are a quasi-linear system with respect to the different LUC processes. Based on this and for simplicity, in the following we will mainly focus on the results using S2 simulations.

Figure 1 shows the time series of simulated $E_{LUC,\ all}$ from all LUC processes (net LUC + land turnover + wood harvest) in comparison with previous studies. Simulated E_{LUC} from each individual LUC process and corresponding time series of LUC areas are shown in Fig. 2. The temporal changes in emissions from S2b simulations are shown in Fig. S7 in the Supplement. All estimations show a gradual increase in E_{LUC} starting from the early 18th century

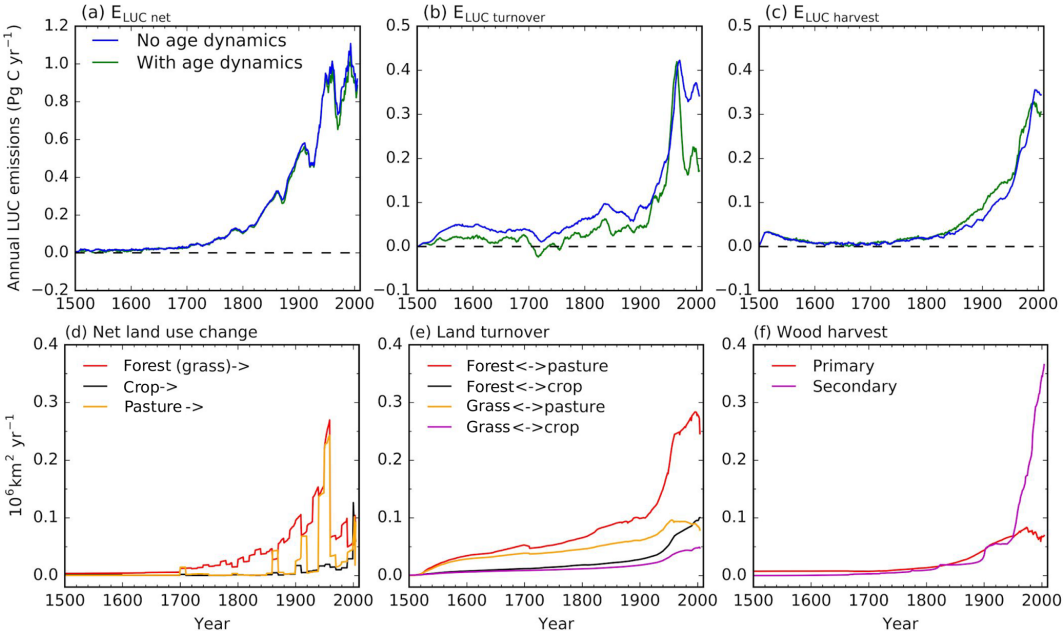

Figure 2. **(a–c)** Annual carbon emissions since 1501 from different LUC processes, **(a)** net land use change, **(b)** land turnover, and **(c)** wood harvest. Data are smoothed using a 10-year average moving window. **(d–f)** Annual time series of areas impacted by different LUC processes. **(d)** Area losses of forest, grassland, cropland, and pasture as a result of net land use change. Note that we assume equal contributions from forest and grassland to agricultural land when backcasting historical land cover maps; thus area losses of forest and grassland are identical. **(e)** Areas subject to land turnover. **(f)** Areas of wood harvest from primary and secondary forests.

with a peak of 1.5–3.5 $\mathrm{Pg\,C\,yr^{-1}}$ around the 1950s, followed by a slight decrease during the 1970s and 1980s and then another peak during the 1990s. E_{LUC} simulated by ORCHIDEE-MICT v8.4.2 is at the lower bound of all estimations until the 1950s, but its second peak of emissions around the 1990s (1.7–1.8 $\mathrm{Pg\,C\,yr^{-1}}$) is a little higher than the first one (1.5 $\mathrm{Pg\,C\,yr^{-1}}$). $E_{\mathrm{LUC\ all,\ ageless}}$ remains slightly higher than $E_{\mathrm{LUC\ all,\ age}}$ until ca. 1960, and after that the difference increases to 0.25 $\mathrm{Pg\,C\,yr^{-1}}$. This two-peak pattern over time in $E_{\mathrm{LUC\ all}}$ by ORCHIDEE-MICT v8.4.2 is mainly driven by $E_{\mathrm{LUC\ net}}$ (Fig. 2a), which also shows two peaks around the 1950s and 1990s, consistent with the peaks of LUC areas in the LUH1 forcing data (Fig. 2d). It should also be noted that as E_{LUC} is quantified as the difference in NBP between two model simulations, its magnitude thus depends on both the areas subject to LUC and the magnitude of carbon fluxes in the reference S0 simulations, as driven by climate variability, atmospheric CO_2, etc.

Consistent with the idealized site-scale simulation in Yue et al. (2018), $E_{\mathrm{LUC\ turnover,\ ageless}}$ is higher than $E_{\mathrm{LUC\ turnvoer,\ age}}$ (Fig. 2b). Emissions from instantaneous fluxes and harvested wood product pool are lower in the S_{age} than in S_{ageless} because in the former case low-biomass secondary forests are converted to agricultural land, as opposed to high-biomass mature forests in the latter one. Similarly, the lower $E_{\mathrm{LUC\ turnvoer}}$ in the S_{age} simulation than S_{ageless} is also found in the results with the S2b simulation (Fig. S7). The difference in $E_{\mathrm{LUC\ turnover}}$ explains most of the difference in $E_{\mathrm{LUC\ all}}$ between S_{age} and S_{ageless} since $E_{\mathrm{LUC\ net}}$ does not differ much (Fig. 2a). The similar estimates of $E_{\mathrm{LUC\ net}}$ are because the cleared forests in net LUC have little difference in their biomass densities between S_{ageless} and S_{age}. Both $E_{\mathrm{LUC\ turnover,\ ageless}}$ and $E_{\mathrm{LUC\ turnover,\ age}}$ roughly follow the temporal pattern of areas impacted by land turnover from LUH1 (Fig. 2e), with a steep increase starting from ca. 1900 until 1980, corresponding to a strong increase in the areas undergoing forest–pasture land turnover. After 1980 the turnover-impacted area stabilizes and then shows a slight decrease. Accordingly, $E_{\mathrm{LUC\ turnover,\ ageless}}$ shows a slight decrease in emissions in Fig. 2b, while $E_{\mathrm{LUC\ turnover,\ age}}$ has a much stronger decrease, driven by the fact that recovering secondary forests gain carbon quickly after being taken out of shifting agriculture systems.

Finally, $E_{\mathrm{LUC\ harvest}}$ values between S_{age} and S_{ageless} simulations are almost identical until 1800 (Fig. 2), during which the wood harvest area remains stable (Fig. 2f). After this, $E_{\mathrm{LUC\ harvest,\ ageless}}$ is lower than $E_{\mathrm{LUC\ harvest,\ age}}$ for the 19th and most of the 20th centuries when $E_{\mathrm{LUC\ harvest}}$ continued to rise, mainly driven by a rise in secondary forest harvest area (Fig. 2f). According to the priority rules of secondary forest harvest in S_{age}, older forests, until the oldest ones, will be harvested if existing young forests cannot meet the prescribed harvest target. This most likely happens when harvested area continues to rise. This exemplifies the potential

inconsistencies between model structure and forcing data. In addition, under such a circumstance, old forests in the S_{age} simulation tend to have higher biomass density than the ageless forests in $S_{ageless}$ because in S_{age} these mature forests remain intact throughout the whole simulation, while in $S_{ageless}$ they are "degraded" due to all kinds of historical LUC activities. This explains the slightly higher $E_{LUC\ harvest}$ in the S_{age} simulation. Similarly, it also explains that the difference in $E_{LUC\ harvest}$ between $S_{ageless}$ and S_{age} from S2b simulations is smaller than that from S2. In S2b simulations, $E_{LUC\ harvest}$ is quantified by including harvest on top of net LUC only, and the harvested forests have not been affected by land turnover, so $E_{LUC\ harvest}$ in the end differs little between $S_{ageless}$ and S_{age}.

3.2 Spatial distribution of LUC emissions

Figure 3 shows the spatial distribution of cumulative E_{LUC} for 1501–2005 from different LUC processes in $S_{ageless}$ (Fig. 3a, d, and g), the difference in E_{LUC} between S_{age} and $S_{ageless}$ (Fig. 3b, e, and h), corresponding net forest area change (Fig. 3c), and areas subject to land turnover (Fig. 3f) and wood harvest (Fig. 3i). The spatial pattern of $E_{LUC\ net}$ generally resembles that of forest area loss, with large areas of forests being cleared and corresponding high $E_{LUC\ net}$ in eastern North America, South America, Africa; southern and eastern Asia; and in central Eurasia (Fig. 3a and c). Central and eastern Europe show some increases in forest area but carbon emissions from net LUC persist, probably because forest recovery happened recently and carbon accumulation in recovering forests is not yet large enough to compensate for historical loss (e.g. see Fig. 5g). Depending on different regions, $E_{LUC\ net,\ age}$ is slightly higher (e.g. along the boreal forest belt in central Europe and Asia, woodland savanna in South America) or lower (e.g. part of Africa and Australia) than $E_{LUC\ net,\ ageless}$ (Fig. 3b). This difference between S_{age} and $S_{ageless}$ is generally small ($< 0.5\,kg\,C\,m^{-2}$ over 1501–2005). It mainly depends on the age classes of forests to be cleared in S_{age} and how the forest biomass density compares with that from $S_{ageless}$ and whether biomass density of the single ageless mature patch is reduced or not with establishment of young forests.

Shifting cultivation is limited to the tropical region (Fig. 3h), as in the original LUH1 forcing data. Tropical Africa is the region with most of the land turnover activities and consequently has the highest $E_{LUC\ turnover}$. Note that the peripheral of the Amazon Basin also shows active shifting cultivations and resulting carbon emissions (Fig. 3b and f). $E_{LUC\ turnover,\ age}$ is in general lower than $E_{LUC\ tunrnover,\ ageless}$ everywhere except at the northern fringe of African woodland savanna (Fig. 3e). Last, wood harvest mainly occurs in temperate and boreal forest in the Northern Hemisphere (Europe and central Siberia, eastern North America, and southern and eastern Asia) and tropical forests including those of the Amazon forest, central Africa, and tropical Asia, with corresponding carbon emissions (Fig. 3c and i). $E_{LUC\ harvest,\ age}$ is a higher source than $E_{LUC\ harvest,\ ageless}$ for most of the harvested regions, which mainly results from the model feature as explained above.

3.3 Simulated regional LUC emissions

Estimated carbon emissions since 1900 from different regions are shown in Fig. 4, with emissions from each LUC source for $S_{ageless}$ being shown in Fig. S8 in the Supplement. The corresponding areas subject to the three LUC processes with forests being mainly involved are shown in Fig. 5. As shown in Fig. 5, in spite of incessant episodic forest gains, for most time in most regions, historical net forest change was dominated by forest loss, except for the second half of the 20th century in western Europe and the former Soviet Union and for the time period after 1970 in the developed Pacific region. Meanwhile, land turnover and wood harvest persisted in most regions, although their magnitudes varied over time. While forest gain can lead to carbon uptake, it could be outweighed by emissions from simultaneous forest loss (note here both forest loss and gain occurred as a result of net LUC within the same region but not within the same grid cell), land turnover, and wood harvest. Thus it is not surprising that LUC impacts on the carbon cycle are diagnosed as emissions in most regions for most of the time, except for the latter half of the 20th century for the former Soviet Union (Fig. 4).

We also compared our estimates with those from Stocker et al. (2014). Stocker et al. (2014) simulated LUC emissions using a different vegetation model (LPX-Bern) but attributed the contributions of each individual LUC process using a similar approach as ours. Both studies are forced by the LUH1 data set, although actual areas undergoing different LUC activities may slightly differ because of different LUC implementation strategies. The two estimates of LUC emissions from our study and Stocker et al. (2014) are in general agreement for most of the regions, including their temporal variations (Fig. 4). Global emissions are dominated by Central and South America, Africa, and the Middle East. Emissions have increased in both regions since 1900, and a peak of emissions occurred around the middle of the 20th century in Africa and around 1980 in Central and South America (Figs. 4a and 5b). Emissions from Stocker et al. (2014) show similar temporal variations in these two regions. The peak of emissions in Africa and the Middle East around 1950 is caused by a peak of forest loss due to net LUC (red line in Fig. 5b) and a surge of forest loss due to land turnover that accelerated between 1940 and 1960 (green line in Fig. 5b). After that emission peak, emissions slightly decreased, mainly due to the stabilized land turnover activities and a drop in area of net LUC. Then the emissions slightly increased again around the 1980s due to an increase in forest loss of net LUC (red line in Fig. 5b) and wood harvest (cyan line in Fig. 5b). In contrast, even with a peak of forest loss due to net LUC

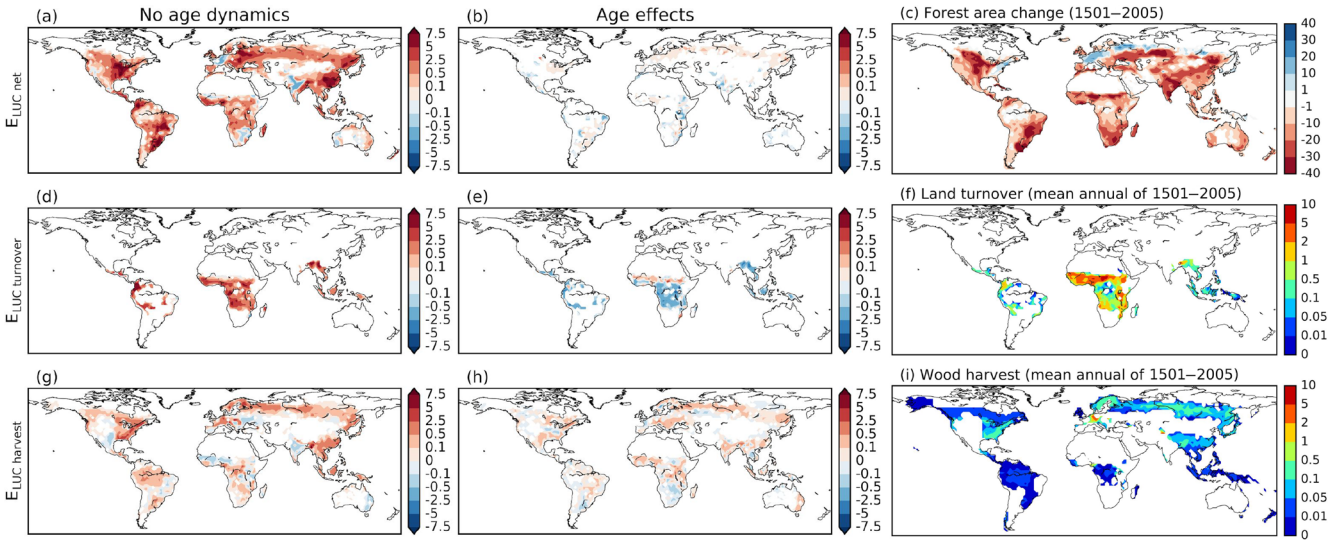

Figure 3. (a–c) Spatial distribution of $E_{\mathrm{LUC\ net}}$ for 1501–2005 ($\mathrm{kg\,C\,m^{-2}}$) as simulated by S_{ageless} simulations, the age effect quantified as difference in $E_{\mathrm{LUC\ net}}$ between S_{age} and S_{ageless}, and the cumulative forest loss as a result of net land use change as a percentage of grid cell area. **(d–f)** Similar to **(a–c)** but for $E_{\mathrm{LUC\ turnover}}$, with **(f)** showing the mean annual grid cell percentage impacted by land turnover over 1501–2005. **(g–i)** Similar to **(a–c)** but for $E_{\mathrm{LUC\ harvest}}$, with **(i)** showing the mean annual grid cell percentage impacted by wood harvest (i.e. sum of wood harvest on primary and secondary forests) over 1501–2005.

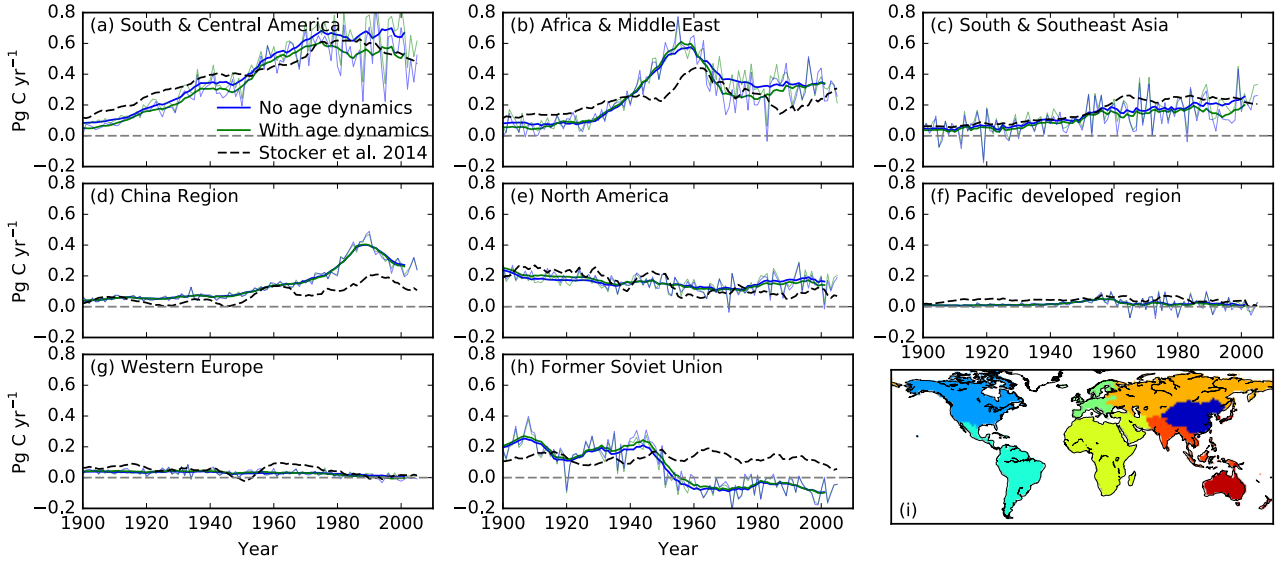

Figure 4. (a–h) Temporal patterns of regional land use change emissions in comparison with those from Stocker et al. (2014). Thicker solid lines indicate annual emissions smoothed using a 10-year moving average from our study, with blue (green) showing emissions from S_{ageless} (S_{age}) simulations. Thinner solid lines indicate unsmoothed annual emissions from our study. Grey dashed lines indicate estimations from Stocker et al. (2014), smoothed using a 10-year moving average. Regional segregation of the globe is shown in **(i)**.

in Central and South America similar to in Africa and the Middle East around the 1950s (red line in Fig. 5a), emissions in the former region continued to increase until the 1980s (Fig. 4a), mainly due to the continuous forest losses resulting from expanding land turnover areas (green line in Fig. 5a).

Both South and Southeast Asia and China showed a steady increase in emissions up to about the 1990s (Fig. 4c and d). In the former region, it is likely driven by continuously growing land turnover and wood harvest; in the latter region, it is more driven by growing net forest loss (Fig. 5c and d). The peak in emissions around the 1990s in China echoes a peak in net forest loss (red line in Fig. 5d). Stocker et al. (2014) show slightly higher emissions than our estimates for South and Southeast Asia and lower magnitude in China, but with sim-

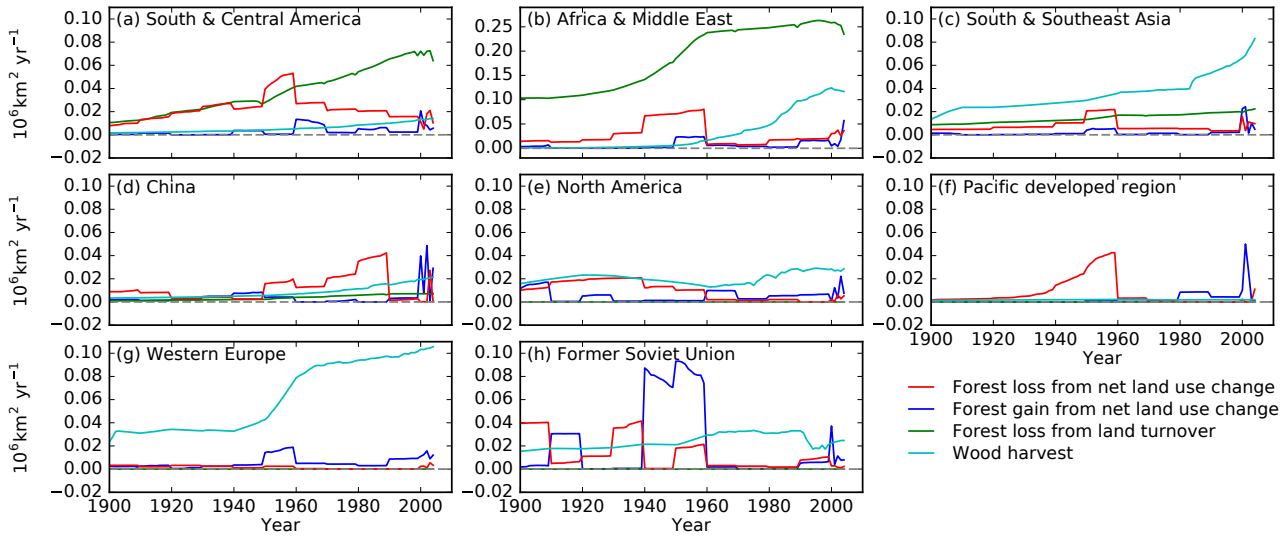

Figure 5. Annual regional areas subject to land use change. Only land use change activities involving forests are assumed to have dominant impacts on E_{LUC} and are thus shown here: forest loss (red line) and gain (blue line) from net land use change, occurring within the same region but not in the same model grid cell; forest involved in land turnover (green line) and wood harvest (cyan line), where forested land remained a forest after land use change. Note that the scale of the y axis in **(b)** is different from the others. See Fig. 4 for the spatial extents of different regions.

ilar temporal patterns in both regions. For the three regions where land turnover activities are included in the LUH1 data set (i.e. Central and South America, Africa and the Middle East, and South and Southeast Asia), there are some periods during which $E_{\mathrm{LUC\ ageless}}$ is clearly higher than $E_{\mathrm{LUC\ age}}$. They mainly correspond to the time when land turnover area either showed decelerated growth or stabilized, roughly after 1970 in Central and South America (Fig. 4a), 1965–1985 in Africa and the Middle East (Fig. 4b), and after 1980 in South and Southeast Asia (Fig. 4c).

North America shows most clearly the legacy impact of past LUC activities on LUC emissions. For the period 1900–1940, carbon emissions in North America gradually decreased even though areas subject to forest loss and wood harvest showed slight increases (Figs. 4e and 5e). This is likely due to the fact that a peak of net forest loss occurred preceding 1900, which yields a high emission legacy for the beginning years of the 20th century (data not shown). LUC emissions and sinks in the developed Pacific region and Europe are very small, despite a high forest wood harvest area in Europe. This is because in general $E_{\mathrm{LUC\ harvest}}$ is small compared to $E_{\mathrm{LUC\ net}}$, probably due to the biomass accumulation in regrowing forest after wood harvest (Fig. S8). The carbon sink as a result of net forest gain is the most prominent in the former Soviet Union (blue line in Fig. 5h), where a peak of forest gain around the 1950s led to a sustained sink of $\sim 0.1\,\mathrm{Pg\,C\,yr^{-1}}$ for the second half of the 20th century (Fig. 4h). However, a concurrent sink is not seen in Stocker et al. (2014) (Fig. 4h).

4 Discussion

4.1 Impacts on estimated E_{LUC} by including gross LUC and sub-grid secondary forests

The advancement in this study in comparison with previous works, as far as we know, is the explicit inclusion of differently aged sub-grid secondary land cohorts in a DGVM. Although secondary lands have been represented in some DGVMs in previous studies (Shevliakova et al., 2009; Stocker et al., 2014; Yang et al., 2010), here we incorporated the concept of rotation cycle. This is particularly important in simulating the carbon cycle impacts of gross LUC, such as wood harvest and shifting cultivation, that often have certain rotation cycles. Because secondary lands, especially young regrowing forests, have lower biomass carbon stock than primary mature forests, the simulated E_{LUC} values involving secondary lands tend to be lower than those from simulations without sub-grid age dynamics. Our results demonstrate that by explicitly including secondary forest cohorts, cumulative E_{LUC} values from shifting cultivation in tropical regions during 1501–2005 are reduced from 45.4 to 27.4 Pg C, or 40 % lower. Nonetheless, it should be noted that these results are based on a constant 15-year rotation length in shifting cultivation, to be consistent with the LUH1 data. To test the sensitivity of $E_{\mathrm{LUC\ turnover}}$ to different rotation lengths in S_{age} simulations, we additionally performed five alternative S2 simulations, all starting from 1861 based on the system state of 1860 obtained from the default S2 simulation, but with the primary target cohort in land turnover varying among the other five cohorts except Cohort_3 (the de-

fault target cohort). The results are presented in Fig. S9 in the Supplement. $E_{\mathrm{LUC\ turnover}}$ over 1861–2005 increases in a roughly linear way with the assumed woody mass of forest cohorts that are cleared in shifting cultivation, with an increase of 5.3 Pg C in emissions per kg C m^{-2} increase in cohort woody mass. $E_{\mathrm{LUC\ turnover,\ ageless}}$ is slightly higher than $E_{\mathrm{LUC\ turnover,\ age}}$ when cohorts with $\sim$ 15 years are cleared primarily. Increasing rotation lengths thus leads to higher emissions than in S_{ageless} simulations in this case. This highlights the importance of the rotation length, i.e. the residence time of agriculture in shifting cultivation systems, for the estimates of $E_{\mathrm{LUC\ turnover}}$.

Table 4 summarized estimates of E_{LUC} from different studies by including both net transitions and gross LUC and the contributions to total emissions by including gross LUC. All studies show that including gross LUC increased estimated carbon emissions. Stocker et al. (2014) reported that gross LUC contributed 15 % to total emissions, whereas Wilkenskjeld et al. (2014) reported a much higher contribution of 38 %. Using a bookkeeping model, Hansis et al. (2015) reported a 22–24 % contribution from gross change if primary lands are cleared, in contrast to a small contribution of only 2 % if secondary lands are cleared. For S_{ageless} in the current study, the contribution of gross LUC to the total emissions is 20 %, falling in between Stocker et al. (2014) and others including the 28 % contribution from gross LUC in the tropics reported by Houghton (2010). However, the simulation including secondary land (i.e. S_{age}) gives a lower gross LUC contribution (15 %) than S_{ageless}. In general, the same model yields a lower contribution of gross changes by converting dominantly secondary land rather than primary land (our study and Hansis et al., 2015). Among different models and methods, the ones including secondary lands (Houghton, 2010; Stocker et al., 2014) tend to yield a lower contribution of gross changes than those that do not (Wilkenskjeld et al., 2014). Although the percentage might differ depending on the amount of gross LUC included and the biomass stocks of the secondary lands being cleared, it seems that contributions from gross LUC are lower when including sub-grid secondary lands.

We also expected E_{LUC} from wood harvest to be smaller when including secondary forests, for the same reason as shifting cultivation. However, we obtained a slightly higher $E_{\mathrm{LUC\ harvest,\ age}}$ than $E_{\mathrm{LUC\ harvest,\ agelss}}$, mainly because there are not enough secondary forests available for harvesting in S_{age}, so that mature forests with a higher biomass density than in S_{ageless} are harvested according to the priority setting in the model, which leads to higher emissions. This model feature was designed to solve the potential inconsistencies between prescribed harvest area in the forcing data and (secondary) forest availability in the model to ensure that ultimately realized harvest area in the model is as close as possible to the prescribed one. From the S2b simulations in which wood harvest, instead of land turnover, is added on top of net LUC, $E_{\mathrm{LUC\ harvest}}$ values derived from S_{age} and S_{ageless} are very similar because in both simulations, forests with biomass close to that of primary forests are harvested. Finally, it should be noted that reconstructions of forest wood harvest are highly uncertain. For example, LUH1 data provide a total wood harvest amount of 102 Pg C for 1850–2005 over forest and non-forest areas, whereas Houghton and Nassikas (2017) estimated 130 Pg C. Our estimates of $E_{\mathrm{LUC\ harvest}}$ using different approaches is 22.5–27.8 Pg for 1850–2005, close to the estimated 25.3 Pg C for 1850–2015 by Houghton and Nassikas (2017).

In the current study, we implemented wood harvest based on input (LUC forcing) information on harvested area rather than on wood volume or biomass. In the future, this process should be modified so that harvested wood volume or biomass information is directly used in the model to allow a dynamic decision on whether an old forest or secondary forest should be harvested. Using wood harvest volume or biomass information would largely alleviate the uncertainty brought about by the unknown wood harvest rotation length because the total amount of harvested biomass would be constrained (Houghton and Nassikas, 2017).

We do not account for any LUC activities in the spin-up run and pristine ecosystems are assumed at the beginning of the transient run in 1501. This set-up might cause a spike in emissions during the beginning years in the transient simulation because ecosystem biomass stocks are high. Such a spike was evident in results by Stocker et al. (2014, blue and green lines in their Fig. 2) when land turnover was not accounted for during the spin-up in some of their simulations. Similar model behaviour is also present in the results by Hansis et al. (2015, dark and light blue lines in their Fig. 4) using a bookkeeping model. In our study, a similar initial spike in E_{LUC} shortly after 1501 is almost invisible for the net LUC and land turnover (Fig. 2a–b), probably owing to very small magnitudes of LUC area within the few years after 1501 (Fig. 2d–e). However, there is a clear peak in $E_{\mathrm{LUC\ turnover}}$ around the 1520s (Fig. 2c), a likely impact of ignoring the spin-up LUC process, given that a significantly larger-than-zero harvest area is prescribed for this period (Fig. 2f). In general, the impacts of not including LUC in the spin-up process seem to be small in our results. This issue impacts the comparisons focusing on emissions starting from 1850 much less (Table 3).

As shown in Fig. 2 and Table 3, our estimations of historical LUC emissions from both S_{ageless} and S_{age} simulations are lower than other studies for most of history (albeit close to Stocker et al., 2014, before ca. 1860). We compared in Table S1 in the Supplement the cumulative E_{LUC} for 1850–2005 from our studies and several previous studies. Our estimates (147 Pg C for $E_{\mathrm{LUC\ age}}$ and 158 Pg C for $E_{\mathrm{LUC\ ageless}}$) are lower than the lower bound of other estimates (171 Pg C by Stocker et al., 2014). Estimations of Hansis et al. (2015) and Gasser and Ciais (2013) using the Hurtt et al. (2011) data set give rather larger estimates than others: 261 and 294 Pg C, respectively. The median value of all previous estimates cited

Table 4. Carbon emissions from gross and net land use transitions and contributions of gross transitions to the total emissions from different studies, adapted from Hansis et al. (2015).

Reference	Time period	E_{LUC} (Pg C)		Contribution of gross transitions, Pg C (%)[d]
		Gross transitions	Net transitions	
This study (S_{age})	1850–2005	147	99	22 (15 %)
This study ($S_{ageless}$)	1850–2005	158	104	31(20 %)
Hansis et al. (2015)[a]	1500–2012	382	374	8.5 (2 %)
Hansis et al. (2015)[b]	1500–2012	382	290	92.4 (24 %)
Hansis et al. (2015)[c]	1500–2012	382	296	85.8 (22 %)
Stocker et al. (2014)	1850–2004	171	146	25 (15 %)
Wilkenskjeld et al. (2014)	1850–2005	225	140	85 (38 %)
Houghton (2010)	1850–2005	156		(28 %, tropics)

[a] Only secondary land is cleared in gross transitions. [b] Primary land is first cleared in gross transitions. [c] Primary land is last cleared in gross transitions. [d] The last column gives the difference in E_{LUC} between gross and net transitions (the absolute value is in Pg C and relative to the net E_{LUC}).

in Table S1 yields 210 Pg C, still much higher than our estimates.

The lower estimates of E_{LUC} in our study are likely linked with underestimated global biomass carbon stock in ORCHIDEE-MICT v8.4.2. The global biomass carbon stock simulated by our model at 1500 prior to any LUC is 365 Pg C and increases to 510 Pg C at 2005 in the S0 simulations (i.e. assuming no LUC activity). The simulated contemporary global biomass in the S3 simulations, in which all three LUC processes are included, remains almost the same as the 1500 value. So the E_{LUC} basically balances out what would have been gained in the global biomass brought about by the environmental changes. Avitabile et al. (2016) have constructed a global contemporary aboveground biomass carbon map by merging two tropical aboveground forest biomass data sets of Saatchi et al. (2011) and Baccini et al. (2012) with Northern Hemisphere volumetric forest stock data from Santoro et al. (2015). Their estimated global forest biomass for aboveground only is 505 Pg C. Our simulated contemporary global total biomass stock (i.e. from S3 simulations) is thus even lower than their estimate for aboveground biomass only. In addition, some of the land transitions in LUH1 data were ignored because of the inconsistencies between LUH1 data and the model PFT map (Sect. 2.2), which may also explain the lower E_{LUC} in our estimation.

4.2 Land use and management processes in DGVMs in relation to forest demography

Forest demography is an important factor in determining forest carbon dynamics on both stand and regional scales (Amiro et al., 2010; Pan et al., 2011). Natural disturbances (such as fire, wind, and insect) and LUC including land management are two primary factors creating spatial heterogeneity in forest age. As more and more forests are now under human management with different intensities (Erb et al., 2017; Luyssaert et al., 2014), sub-grid forest demography should be incorporated in DGVMs to account for the management consequences. Furthermore, when making a more accurate (and detailed) account of regional carbon balances with LUC, other land cover types than forests should be distinguished into different cohorts as well because the presence of many nonlinear processes (e.g. soil carbon decomposition) makes the simple averaging scheme – as in the case in which they are represented with a single patch within the model – a suboptimal choice. This new model structure to have more than one cohort for the same land cover within a grid cell, as has also been explored by Shevliakova et al. (2009), will have an impact on simulated biogeochemical and biophysical processes.

However, despite these improvements in model structure, it remains a big challenge to "seamlessly" integrate LUC forcing data into the model. The fundamental reason is that historical transitions of LUC are not reconstructed in a way that is internally consistent with DGVMs. The systems to build historical LUC transitions (so-called land use models) and DGVMs may use different land cover types so that conciliating the two land cover maps is inevitable. This will lead to loss of information in incorporating forcing data into the model, as is also pointed out by Stocker et al. (2014). Second, simulated forest biomass density might be different as well; therefore the same amount of harvested wood volume may be translated into different forest areas in land use models and DGVMs. Recently progress has been made in DGVMs to represent forest stand structure and detailed management options (Naudts et al., 2015), so that harvested wood volume as a model output can be validated with statistical data. Third, the rotation length of shifting cultivation or forest management used in DGVMs may not be consistent with that assumed in land use models.

To overcome these obstacles and to promote a more comprehensive integration of LUC information into DGVMs,

Table 5. Nomenclature.

LUC:	land use change
E_{LUC}:	carbon emissions from land use change. Positive values indicate that LUC has a net effect of releasing carbon from land to the atmosphere, while a negative value indicates the reverse.
$E_{\mathrm{LUC\ process[,\ configuration]}}$:	carbon emissions from a certain LUC process (net transitions only, land turnover, wood harvest, or all three processes combined) quantified by a specific model configuration (age or ageless, in which differently aged sub-grid land cohorts are or are not explicitly represented, respectively). For instance, $E_{\mathrm{LUC\ net,\ ageless}}$ indicates E_{LUC} from net transitions only and without explicitly representing sub-grid age dynamics, i.e. a single ageless mature patch is used to represent a land cover type; $E_{\mathrm{LUC\ net,\ age}}$ indicates E_{LUC} from the same process using a model configuration that explicitly represents differently aged land cohorts.
$\mathrm{S_{age}}$:	model simulations that represent sub-grid secondary land cohorts.
$\mathrm{S_{ageless}}$:	model simulations that do not include sub-grid age dynamics, i.e. a single ageless mature patch is used to represent a land cover type.

one possible route is to further develop DGVMs to partly embed functions of land use models. This will allow DGVMs to be used in a manner "inversed" from its current utilization. For example, food demand could be used as an input, so that dynamical decisions could be made within the model on how many croplands need to be created given the simulated crop yield by the crop module inside the DGVM. The same case also applies to pasture. Grassland management modules within DGVMs could generate information on meat and milk production etc., and this information could be used to inverse the meat and milk demand into demanded pasture areas (Chang et al., 2016). Harvested wood for a certain product usage might need wood with a specific diameter range, corresponding to a certain forest age class given its simulated growth state, allowing the determination of both ages and areas of forests to be harvested.

5 Conclusions

In this study, we investigated the impacts on estimated historical gross LUC emissions by accounting for multiple sub-grid secondary land cohorts in a DGVM. The model employed here is capable of representing the rotation processes in land use and land management that mainly involve secondary forests, such as shifting cultivation and forest wood harvest. Intermediately aged secondary forests are given a high priority when forest clearing occurs in either shifting cultivation or wood harvest, complemented by older forests if young ones are insufficient to meet the prescribed land use transition. For the net LUC, clearing of forests starts exclusively from mature forests and moves sequentially to younger forests when older ones are used up. This set of rules becomes indispensable when incorporating multiple sub-grid secondary land cohorts and reconciling with external land use transition forcing data in the model. As such, the simulated portfolio of secondary land cohorts within the model is driven by a reconstruction of historical gross LUC.

Following the input data of land use transition reconstruction, we assumed a constant shifting cultivation rotation length of 15 years in the tropics. We found that over 1501–2005, accounting for sub-grid secondary land cohorts yields a lower E_{LUC} (176 vs. 197 Pg C), which is dominated by lower emissions from shifting cultivation (27 vs. 46 Pg C or 40 % lower in the former case). This is because secondary forests with a lower biomass are allowed to be cleared, instead of the mature forests with a high biomass as in the approach representing only mature forest in DGVMs. The lower emissions from shifting cultivation when accounting for sub-grid multiple land cohorts highly depend on the assumed rotation length. A set of sensitivity runs for Africa showed that a longer historical shifting cultivation rotation length leads to higher associated emissions. This highlights the need for more reliable reconstructions of the areas as well as the historical rotation lengths of shifting cultivation to reduce uncertainty on E_{LUC}. Our results show that although gross LUC as a previously neglected LUC emission component has been included by a growing number of DGVMs, its contribution to overall E_{LUC} remains uncertain and tends to be overestimated by models ignoring sub-grid secondary forests.

Data availability. All data used to generate the figures are available upon request to the corresponding author.

The Supplement related to this article is available online at https://doi.org/10.5194/bg-15-1185-2018-supplement.

Competing interests. The authors declare that they have no conflict of interest.

Acknowledgements. Chao Yue, Philippe Ciais, and Wei Li acknowledge support from the European Research Council through Synergy grant ERC-2013-SyG-610028 "IMBALANCE-P". Wei Li and Chao Yue are also supported by the European Commission-funded project LUC4C (no. 603542). The authors thank the two reviewers for their constructive comments that help to improve the paper quality.

Edited by: Victor Brovkin
Reviewed by: Benjamin Stocker and one anonymous referee

References

Amiro, B. D., Barr, A. G., Barr, J. G., Black, T. A., Bracho, R., Brown, M., Chen, J., Clark, K. L., Davis, K. J., Desai, A. R., Dore, S., Engel, V., Fuentes, J. D., Goldstein, A. H., Goulden, M. L., Kolb, T. E., Lavigne, M. B., Law, B. E., Margolis, H. A., Martin, T., McCaughey, J. H., Misson, L., Montes-Helu, M., Noormets, A., Randerson, J. T., Starr, G., and Xiao, J.: Ecosystem carbon dioxide fluxes after disturbance in forests of North America, J. Geophys. Res., 115, G00K02, https://doi.org/10.1029/2010JG001390, 2010.

Arneth, A., Sitch, S., Pongratz, J., Stocker, B. D., Ciais, P., Poulter, B., Bayer, A. D., Bondeau, A., Calle, L., Chini, L. P., Gasser, T., Fader, M., Friedlingstein, P., Kato, E., Li, W., Lindeskog, M., Nabel, J. E. M. S., Pugh, T. a. M., Robertson, E., Viovy, N., Yue, C., and Zaehle, S.: Historical carbon dioxide emissions caused by land-use changes are possibly larger than assumed, Nat. Geosci., 10, 79–84, https://doi.org/10.1038/ngeo2882, 2017.

Avitabile, V., Herold, M., Heuvelink, G. B. M., Lewis, S. L., Phillips, O. L., Asner, G. P., Armston, J., Ashton, P. S., Banin, L., Bayol, N., Berry, N. J., Boeckx, P., de Jong, B. H. J., DeVries, B., Girardin, C. A. J., Kearsley, E., Lindsell, J. A., Lopez-Gonzalez, G., Lucas, R., Malhi, Y., Morel, A., Mitchard, E. T. A., Nagy, L., Qie, L., Quinones, M. J., Ryan, C. M., Ferry, S. J. W., Sunderland, T., Laurin, G. V., Gatti, R. C., Valentini, R., Verbeeck, H., Wijaya, A., and Willcock, S.: An integrated pan-tropical biomass map using multiple reference datasets, Glob. Change Biol., 22, 1406–1420, https://doi.org/10.1111/gcb.13139, 2016.

Baccini, A., Goetz, S. J., Walker, W. S., Laporte, N. T., Sun, M., Sulla-Menashe, D., Hackler, J., Beck, P. S. A., Dubayah, R., Friedl, M. A., Samanta, S., and Houghton, R. A.: Estimated carbon dioxide emissions from tropical deforestation improved by carbon-density maps, Nat. Clim. Change, 2, 182–185, https://doi.org/10.1038/nclimate1354, 2012.

Bayer, A. D., Lindeskog, M., Pugh, T. A. M., Anthoni, P. M., Fuchs, R., and Arneth, A.: Uncertainties in the land-use flux resulting from land-use change reconstructions and gross land transitions, Earth Syst. Dynam., 8, 91–111, https://doi.org/10.5194/esd-8-91-2017, 2017.

Chang, J., Ciais, P., Herrero, M., Havlik, P., Campioli, M., Zhang, X., Bai, Y., Viovy, N., Joiner, J., Wang, X., Peng, S., Yue, C., Piao, S., Wang, T., Hauglustaine, D. A., Soussana, J.-F., Peregon, A., Kosykh, N., and Mironycheva-Tokareva, N.: Combining livestock production information in a process-based vegetation model to reconstruct the history of grassland management, Biogeosciences, 13, 3757–3776, https://doi.org/10.5194/bg-13-3757-2016, 2016.

Chazdon, R. L., Broadbent, E. N., Rozendaal, D. M. A., Bongers, F., Zambrano, A. M. A., Aide, T. M., Balvanera, P., Becknell, J. M., Boukili, V., Brancalion, P. H. S., Craven, D., Almeida-Cortez, J. S., Cabral, G. A. L., Jong, B. de, Denslow, J. S., Dent, D. H., DeWalt, S. J., Dupuy, J. M., Durán, S. M., Espírito-Santo, M. M., Fandino, M. C., César, R. G., Hall, J. S., Hernández-Stefanoni, J. L., Jakovac, C. C., Junqueira, A. B., Kennard, D., Letcher, S. G., Lohbeck, M., Martínez-Ramos, M., Massoca, P., Meave, J. A., Mesquita, R., Mora, F., Muñoz, R., Muscarella, R., Nunes, Y. R. F., Ochoa-Gaona, S., Orihuela-Belmonte, E., Peña-Claros, M., Pérez-García, E. A., Piotto, D., Powers, J. S., Rodríguez-Velazquez, J., Romero-Pérez, I. E., Ruíz, J., Saldarriaga, J. G., Sanchez-Azofeifa, A., Schwartz, N. B., Steininger, M. K., Swenson, N. G., Uriarte, M., Breugel, M. van, Wal, H. van der, Veloso, M. D. M., Vester, H., Vieira, I. C. G., Bentos, T. V., Williamson, G. B., and Poorter, L.: Carbon sequestration potential of second-growth forest regeneration in the Latin American tropics, Sci. Adv., 2, e1501639, https://doi.org/10.1126/sciadv.1501639, 2016.

Don, A., Schumacher, J., and Freibauer, A.: Impact of tropical land-use change on soil organic carbon stocks – a meta-analysis, Glob. Change Biol., 17, 1658–1670, https://doi.org/10.1111/j.1365-2486.2010.02336.x, 2011.

Erb, K.-H., Luyssaert, S., Meyfroidt, P., Pongratz, J., Don, A., Kloster, S., Kuemmerle, T., Fetzel, T., Fuchs, R., Herold, M., Haberl, H., Jones, C. D., Marín-Spiotta, E., McCallum, I., Robertson, E., Seufert, V., Fritz, S., Valade, A., Wiltshire, A., and Dolman, A. J.: Land management: data availability and process understanding for global change studies, Glob. Change Biol., 23, 512–533, https://doi.org/10.1111/gcb.13443, 2017.

Gasser, T. and Ciais, P.: A theoretical framework for the net land-to-atmosphere CO_2 flux and its implications in the definition of "emissions from land-use change", Earth Syst. Dynam., 4, 171–186, https://doi.org/10.5194/esd-4-171-2013, 2013.

Hansis, E., Davis, S. J., and Pongratz, J.: Relevance of methodological choices for accounting of land use change carbon fluxes, Global Biogeochem. Cy., 29, 2014GB004997, https://doi.org/10.1002/2014GB004997, 2015.

Houghton, R. A.: The annual net flux of carbon to the atmosphere from changes in land use 1850–1990, Tellus B, 51, 298–313, https://doi.org/10.1034/j.1600-0889.1999.00013.x, 1999.

Houghton, R. A.: Revised estimates of the annual net flux of carbon to the atmosphere from changes in land use and land management 1850–2000, Tellus B, 55, 378–390, https://doi.org/10.1034/j.1600-0889.2003.01450.x, 2003.

Houghton, R. A.: How well do we know the flux of CO_2 from land-use change?, Tellus B, 62, 337–351, https://doi.org/10.1111/j.1600-0889.2010.00473.x, 2010.

Houghton, R. A. and Nassikas, A. A.: Global and regional fluxes of carbon from land use and land cover change 1850–2015, Global Biogeochem. Cy., 31, 2016GB005546, https://doi.org/10.1002/2016GB005546, 2017.

Hurtt, G. C., Chini, L. P., Frolking, S., Betts, R. A., Feddema, J., Fischer, G., Fisk, J. P., Hibbard, K., Houghton, R. A., Janetos, A., Jones, C. D., Kindermann, G., Kinoshita, T., Goldewijk, K. K., Riahi, K., Shevliakova, E., Smith, S., Stehfest, E., Thomson, A., Thornton, P., Vuuren, D. P. van and Wang, Y. P.: Harmonization of land-use scenarios for the period 1500–2100: 600 years of global gridded annual land-use transitions, wood harvest, and resulting secondary lands, Climatic Change, 109, 117, https://doi.org/10.1007/s10584-011-0153-2, 2011.

Kato, E., Kinoshita, T., Ito, A., Kawamiya, M., and Yamagata, Y.: Evaluation of spatially explicit emission scenario of land-use change and biomass burning using a process-based biogeochemical model, J. Land Use Sci., 8, 104–122, https://doi.org/10.1080/1747423X.2011.628705, 2013.

Krinner, G., Viovy, N., de Noblet-Ducoudré, N., Ogée, J., Polcher, J., Friedlingstein, P., Ciais, P., Sitch, S., and Prentice, I. C.: A dynamic global vegetation model for studies of the coupled atmosphere–biosphere system, Global Biogeochem. Cy., 19, GB1015, https://doi.org/10.1029/2003GB002199, 2005.

Le Quéré, C., Andrew, R. M., Canadell, J. G., Sitch, S., Korsbakken, J. I., Peters, G. P., Manning, A. C., Boden, T. A., Tans, P. P., Houghton, R. A., Keeling, R. F., Alin, S., Andrews, O. D., Anthoni, P., Barbero, L., Bopp, L., Chevallier, F., Chini, L. P., Ciais, P., Currie, K., Delire, C., Doney, S. C., Friedlingstein, P., Gkritzalis, T., Harris, I., Hauck, J., Haverd, V., Hoppema, M., Klein Goldewijk, K., Jain, A. K., Kato, E., Körtzinger, A., Landschützer, P., Lefèvre, N., Lenton, A., Lienert, S., Lombardozzi, D., Melton, J. R., Metzl, N., Millero, F., Monteiro, P. M. S., Munro, D. R., Nabel, J. E. M. S., Nakaoka, S.-I., O'Brien, K., Olsen, A., Omar, A. M., Ono, T., Pierrot, D., Poulter, B., Rödenbeck, C., Salisbury, J., Schuster, U., Schwinger, J., Séférian, R., Skjelvan, I., Stocker, B. D., Sutton, A. J., Takahashi, T., Tian, H., Tilbrook, B., van der Laan-Luijkx, I. T., van der Werf, G. R., Viovy, N., Walker, A. P., Wiltshire, A. J., and Zaehle, S.: Global Carbon Budget 2016, Earth Syst. Sci. Data, 8, 605–649, https://doi.org/10.5194/essd-8-605-2016, 2016.

Li, W., MacBean, N., Ciais, P., Defourny, P., Lamarche, C., Bontemps, S., Houghton, R. A., and Peng, S.: Gross and net land cover changes in the main plant functional types derived from the annual ESA CCI land cover maps (1992–2015), Earth Syst. Sci. Data, 10, 219–234, https://doi.org/10.5194/essd-10-219-2018, 2018.

Luyssaert, S., Jammet, M., Stoy, P. C., Estel, S., Pongratz, J., Ceschia, E., Churkina, G., Don, A., Erb, K., Ferlicoq, M., Gielen, B., Grünwald, T., Houghton, R. A., Klumpp, K., Knohl, A., Kolb, T., Kuemmerle, T., Laurila, T., Lohila, A., Loustau, D., McGrath, M. J., Meyfroidt, P., Moors, E. J., Naudts, K., Novick, K., Otto, J., Pilegaard, K., Pio, C. A., Rambal, S., Rebmann, C., Ryder, J., Suyker, A. E., Varlagin, A., Wattenbach, M., and Dolman, A. J.: Land management and land-cover change have impacts of similar magnitude on surface temperature, Nat. Clim. Change, 4, 389–393, https://doi.org/10.1038/nclimate2196, 2014.

McGrath, M. J., Luyssaert, S., Meyfroidt, P., Kaplan, J. O., Bürgi, M., Chen, Y., Erb, K., Gimmi, U., McInerney, D., Naudts, K., Otto, J., Pasztor, F., Ryder, J., Schelhaas, M.-J., and Valade, A.: Reconstructing European forest management from 1600 to 2010, Biogeosciences, 12, 4291–4316, https://doi.org/10.5194/bg-12-4291-2015, 2015.

Meiyappan, P. and Jain, A. K.: Three distinct global estimates of historical land-cover change and land-use conversions for over 200 years, Front. Earth Sci., 6, 122–139, https://doi.org/10.1007/s11707-012-0314-2, 2012.

Naudts, K., Ryder, J., McGrath, M. J., Otto, J., Chen, Y., Valade, A., Bellasen, V., Berhongaray, G., Bönisch, G., Campioli, M., Ghattas, J., De Groote, T., Haverd, V., Kattge, J., MacBean, N., Maignan, F., Merilä, P., Penuelas, J., Peylin, P., Pinty, B., Pretzsch, H., Schulze, E. D., Solyga, D., Vuichard, N., Yan, Y., and Luyssaert, S.: A vertically discretised canopy description for ORCHIDEE (SVN r2290) and the modifications to the energy, water and carbon fluxes, Geosci. Model Dev., 8, 2035–2065, https://doi.org/10.5194/gmd-8-2035-2015, 2015.

Pan, Y., Chen, J. M., Birdsey, R., McCullough, K., He, L., and Deng, F.: Age structure and disturbance legacy of North American forests, Biogeosciences, 8, 715–732, https://doi.org/10.5194/bg-8-715-2011, 2011.

Peng, S., Ciais, P., Maignan, F., Li, W., Chang, J., Wang, T., and Yue, C.: Sensitivity of land use change emission estimates to historical land use and land cover mapping, Global Biogeochem. Cy., 31, 2015GB005360, https://doi.org/10.1002/2015GB005360, 2017.

Piao, S., Ciais, P., Friedlingstein, P., de Noblet-Ducoudré, N., Cadule, P., Viovy, N., and Wang, T.: Spatiotemporal patterns of terrestrial carbon cycle during the 20th century, Global Biogeochem. Cy., 23, GB4026, https://doi.org/10.1029/2008GB003339, 2009a.

Piao, S., Fang, J., Ciais, P., Peylin, P., Huang, Y., Sitch, S., and Wang, T.: The carbon balance of terrestrial ecosystems in China, Nature, 458, 1009–1013, https://doi.org/10.1038/nature07944, 2009b.

Poeplau, C., Don, A., Vesterdal, L., Leifeld, J., Van Wesemael, B., Schumacher, J., and Gensior, A.: Temporal dynamics of soil organic carbon after land-use change in the temperate zone – carbon response functions as a model approach, Glob. Change Biol., 17, 2415–2427, https://doi.org/10.1111/j.1365-2486.2011.02408.x, 2011.

Pongratz, J., Reick, C. H., Raddatz, T., and Claussen, M.: Effects of anthropogenic land cover change on the carbon cycle of the last millennium, Global Biogeochem. Cy., 23, GB4001, https://doi.org/10.1029/2009GB003488, 2009.

Poorter, L., Bongers, F., Aide, T. M., Almeyda Zambrano, A. M., Balvanera, P., Becknell, J. M., Boukili, V., Brancalion, P. H. S., Broadbent, E. N., Chazdon, R. L., Craven, D., de Almeida-Cortez, J. S., Cabral, G. A. L., de Jong, B. H. J., Denslow, J. S., Dent, D. H., DeWalt, S. J., Dupuy, J. M., Durán, S. M., Espírito-Santo, M. M., Fandino, M. C., César, R. G., Hall, J. S., Hernandez-Stefanoni, J. L., Jakovac, C. C., Junqueira, A. B., Kennard, D., Letcher, S. G., Licona, J.-C., Lohbeck, M., Marín-Spiotta, E., Martínez-Ramos, M., Massoca, P., Meave, J. A., Mesquita, R., Mora, F., Muñoz, R., Muscarella, R., Nunes, Y. R. F., Ochoa-Gaona, S., de Oliveira, A. A., Orihuela-Belmonte, E., Peña-Claros, M., Pérez-García, E. A., Piotto, D., Powers, J. S., Rodríguez-Velázquez, J., Romero-Pérez, I. E., Ruíz, J., Saldarriaga, J. G., Sanchez-Azofeifa, A., Schwartz, N. B., Steininger, M. K., Swenson, N. G., Toledo, M., Uriarte, M., van Breugel, M., van der Wal, H., Veloso, M. D. M.,

Vester, H. F. M., Vicentini, A., Vieira, I. C. G., Bentos, T. V., Williamson, G. B., and Rozendaal, D. M. A.: Biomass resilience of neotropical secondary forests, Nature, 530, 211–214, https://doi.org/10.1038/nature16512, 2016.

Saatchi, S. S., Harris, N. L., Brown, S., Lefsky, M., Mitchard, E. T. A., Salas, W., Zutta, B. R., Buermann, W., Lewis, S. L., Hagen, S., Petrova, S., White, L., Silman, M., and Morel, A.: Benchmark map of forest carbon stocks in tropical regions across three continents, P. Natl. Acad. Sci. USA, 108, https://doi.org/10.1073/pnas.1019576108, 2011.

Santoro, M., Beaudoin, A., Beer, C., Cartus, O., Fransson, J. E. S., Hall, R. J., Pathe, C., Schmullius, C., Schepaschenko, D., Shvidenko, A., Thurner, M., and Wegmüller, U.: Forest growing stock volume of the Northern Hemisphere: spatially explicit estimates for 2010 derived from Envisat ASAR, Remote Sens. Environ., 168, 316–334, https://doi.org/10.1016/j.rse.2015.07.005, 2015.

Shevliakova, E., Pacala, S. W., Malyshev, S., Hurtt, G. C., Milly, P. C. D., Caspersen, J. P., Sentman, L. T., Fisk, J. P., Wirth, C., and Crevoisier, C.: Carbon cycling under 300 years of land use change: importance of the secondary vegetation sink, Global Biogeochem. Cy., 23, GB2022, https://doi.org/10.1029/2007GB003176, 2009.

Smith, B., Prentice, I. C., and Sykes, M. T.: Representation of vegetation dynamics in the modelling of terrestrial ecosystems: comparing two contrasting approaches within European climate space, Global Ecol. Biogeogr., 10, 621–637, https://doi.org/10.1046/j.1466-822X.2001.t01-1-00256.x, 2001.

Stocker, B. D., Feissli, F., Strassmann, K. M., Spahni, R., and Joos, F.: Past and future carbon fluxes from land use change, shifting cultivation and wood harvest, Tellus B, 66, 621–637, https://doi.org/10.3402/tellusb.v66.23188, 2014.

van der Werf, G. R., Randerson, J. T., Giglio, L., Collatz, G. J., Mu, M., Kasibhatla, P. S., Morton, D. C., DeFries, R. S., Jin, Y., and van Leeuwen, T. T.: Global fire emissions and the contribution of deforestation, savanna, forest, agricultural, and peat fires (1997–2009), Atmos. Chem. Phys., 10, 11707–11735, https://doi.org/10.5194/acp-10-11707-2010, 2010.

van Vliet, N., Mertz, O., Heinimann, A., Langanke, T., Pascual, U., Schmook, B., Adams, C., Schmidt-Vogt, D., Messerli, P., Leisz, S., Castella, J.-C., Jørgensen, L., Birch-Thomsen, T., Hett, C., Bech-Bruun, T., Ickowitz, A., Vu, K. C., Yasuyuki, K., Fox, J., Padoch, C., Dressler, W., and Ziegler, A. D.: Trends, drivers and impacts of changes in swidden cultivation in tropical forest-agriculture frontiers: a global assessment, Global Environ. Chang., 22, 418–429, https://doi.org/10.1016/j.gloenvcha.2011.10.009, 2012.

Wilkenskjeld, S., Kloster, S., Pongratz, J., Raddatz, T., and Reick, C. H.: Comparing the influence of net and gross anthropogenic land-use and land-cover changes on the carbon cycle in the MPI-ESM, Biogeosciences, 11, 4817–4828, https://doi.org/10.5194/bg-11-4817-2014, 2014.

Yang, X., Richardson, T. K., and Jain, A. K.: Contributions of secondary forest and nitrogen dynamics to terrestrial carbon uptake, Biogeosciences, 7, 3041–3050, https://doi.org/10.5194/bg-7-3041-2010, 2010.

Yue, C., Ciais, P., Cadule, P., Thonicke, K., Archibald, S., Poulter, B., Hao, W. M., Hantson, S., Mouillot, F., Friedlingstein, P., Maignan, F., and Viovy, N.: Modelling the role of fires in the terrestrial carbon balance by incorporating SPITFIRE into the global vegetation model ORCHIDEE – Part 1: simulating historical global burned area and fire regimes, Geosci. Model Dev., 7, 2747–2767, https://doi.org/10.5194/gmd-7-2747-2014, 2014.

Yue, C., Ciais, P., Luyssaert, S., Li, W., McGrath, M. J., Chang, J., and Peng, S.: Representing anthropogenic gross land use change, wood harvest, and forest age dynamics in a global vegetation model ORCHIDEE-MICT v8.4.2, Geosci. Model Dev., 11, 409–428, https://doi.org/10.5194/gmd-11-409-2018, 2018.